Indian Journal of Marine Sciences
Vol. 33(2), June 2004, pp 150-154

Long period waves in the coastal regions of north Indian Ocean

*P V Hareesh Kumar & K V Sanilkumar
Naval Physical & Oceanographic Laboratory, Kochi – 682 021, India
[*E-mail: tsonpol@vsnl.com]

Received 17 March 2003, revised 9 February 2004

The sea surface height (SSH) anomaly derived from TOPEX/POSEIDON altimeter was used to study the characteristics of long period waves in the coastal belt of north Indian Ocean. Wavelet analysis at typical locations revealed that the most dominant signals were in the bands of intra-seasonal oscillation (ISO), i.e. 30-60 days, 3-4 months, semi-annual and annual. Among them, the annual signal contained maximum energy at all the locations. But, inside the Andaman Sea, and off the Gulf of Aden, the ISO component is of nearly equal magnitude as that of annual. In the regions of large SSH variability, low frequency components (more than 3 months) dominated, whereas they contained less energy in the region of minimum SSH variability. Hovmullor diagrams revealed large inter- and intra-annual variability in the SSH fields. In general, along the eastern boundary of the ocean, high sea level was observed during April-June and October-December in association with equatorial Kelvin waves. Another notable observation was the formation of high SSH in the western Indian Ocean during February-May and August-October. Among them, the former one propagated northward while latter one was found stationary. The Markan coast was found as the region of meeting place of two waves, one from the western Indian Ocean and the other from the eastern Bay. The results can be utilized to enhance the understanding of various coastal processes controlled by long period waves, viz. upwelling, sinking, circulation and meso-scale features.

[**Key words**: Long period waves, coastal waters, sea surface height anomaly, intra-seasonal oscillation, wavelet analysis]

Introduction

Recent studies show that long period waves play a vital role in controlling the dynamics of the north Indian Ocean[1-3]. Among these waves, the dominant ones are Rossby waves, Kelvin waves, Yanai waves etc. Sudden change in the wind system in the equatorial Indian Ocean during the pre- and post-monsoon seasons generate eastward propagating Kelvin waves and take nearly one month to reach the eastern Indian Ocean[4-6]. This in turn causes high sea levels in the eastern boundary. On encountering the eastern boundary, part of the Kelvin wave's energy is reflected back to the equatorial wave-guide as Rossby waves, while the remaining energy forms coastally trapped Kelvin waves. As these waves propagate pole ward, they excite Rossby waves with the same frequency into the interior ocean. Most of the studies[5-7] dealt with the formation and propagation of these waves in the interior Indian Ocean. These studies have also clearly demonstrated these waves play an influential part in the generation and propagation of eddies in the ocean. Recently, Hareesh Kumar *et al.*[8] reported that the waves with intra-seasonal periodicity influence the upper ocean dynamics in the Bay of Bengal during summer monsoon season rather than the local forcing. In spite of these importances, not many studies were carried out to understand the characteristics of these waves in the Indian waters, especially in the coastal regions, where the dynamics are more complex. Hence, in this paper, we explicitly concentrate along the coastal belt of the north Indian Ocean to study characteristics of these waves. Moreover, the wavelet decomposition method to identify the prominent harmonics was utilized for the first time in the Indian coastal regions.

Data

The processed SSH data obtained from TOPEX/ POSEIDON team (WOCE Data products Committee, Jet Propulsion Laboratory, USA, 1998) for the period 1993-97 was utilized in this study. Data within the coastal regions (i.e. up to 1^o away from the coast) of the north Indian Ocean (Fig. 1) was sorted out and averaged for the grids of $0.5^o \times 1^o$ (latitude by longitude) size all along the coast. As the offshore length scale of the coastal Rossby wave varies with latitude, a length scale of 1^o was chosen[3]. The grids start from off Somalia (0^o, 46.5^o E) and end off Sumatra (1.5^oN, 95^oE) and were numbered in serial

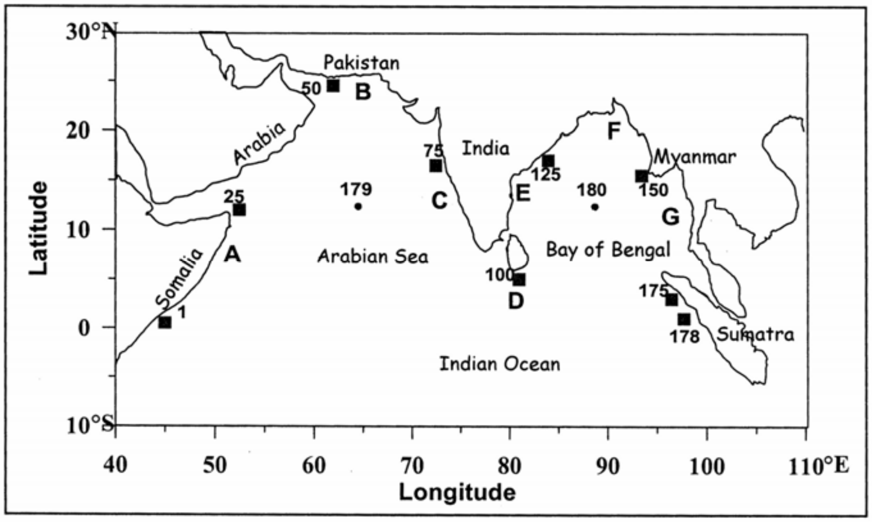

Fig. 1—Area map. Numbers 1 to 180 represents the grids of size $0.5^o \times 1^o$ (latitude by longitude) from Somalia to Sumatra along the entire coastal belt. A to G represents various selected regions

order. In addition, time series of SSH at two locations, sorted from the processed SSH data, representing the central Arabian Sea (12^{o}N, 64.5^{o}E) and central Bay of Bengal (12^{o}N, 88.5^{o}E) were also utilized to compare and contrast between the coastal and deep waters.

Results and Discussion

Sea level variability along the coastal belt is controlled by upwelling/ downwelling, river discharges, winds, currents, tides and long period waves etc. The SSH data obtained from altimeter include the combined effect of all these factors, which are highly location and time specific. In order to understand the variability of sea level in the coastal regions, SSH values for all the grids were plotted (Fig. 2). In general, minimum temporal variation in SSH (i.e. minimum scatter) was observed off Somalia (grid 1-3), Makran (Fig. 2, B) and Sri Lanka (Fig. 2, D). Among them, the least variations occurred at grid 52 in the region B (-100 to 100 mm). On the other hand, in the coastal regions of Bay of Bengal (Fig. 2, E, F and G) and off Gulf of Aden (at grid 25 in the region A), maximum SSH variations (-400 to 300 mm) were observed. Here it is interesting to note that the spread decreased towards both sides from grid 25 (i.e. to grid 1 and 52 respectively). Similarly, off the west coast of India (C) also, the spread (-250 to 250 mm) decreased from the southern tip of India (grid 89) towards both sides (i.e. towards region B and D). These observations clearly indicated that large spatio-temporal variations occur in sea level in the coastal waters of the north Indian Ocean.

To understand the evolution of SSH along the coastal boundaries, the time series of SSH for the years 1993 to 1997 were sorted for each grid, and the Hovmullor diagram was prepared (Fig. 3). The figure revealed large intra- and inter-annual variability in SSH in the entire coastal belt, as evident from the appearance of high (yellow-red patch) and low (blue patch). In general, along the eastern boundary of the ocean, sea level was high during April-June and October-December and low during January-March and July-October. However, during the years 1994 and 1997, more number of intermittent lows and highs of short period appeared which might have suppressed the well-defined high. This feature was evident in the other grids also. It is to be noted that these years were El-Nino years.

The Hovmuller diagram (Fig. 3) clearly indicated the propagation of a coastal Kelvin wave from Sumatra to the head Bay and southern tip of India to the Makran coast. It also indicated the propagation of a wave from Somalia to the Makran coast on the west Arabian Sea. The appearance of high in the eastern Bay of Bengal twice in a year, one during April and the other during October was due to the arrival of equatorial Kelvin waves in the eastern Bay, generated due to collapse of north-easterly winds during mid February and south-westerly winds during September. These highs and lows in the eastern Bay propagate to the lower grids as coastally trapped Kelvin waves. Moreover, it is reported that this Kelvin wave radiates energy as Rossby waves as they propagate poleward[1,7,9]. The high formed in the eastern Arabian

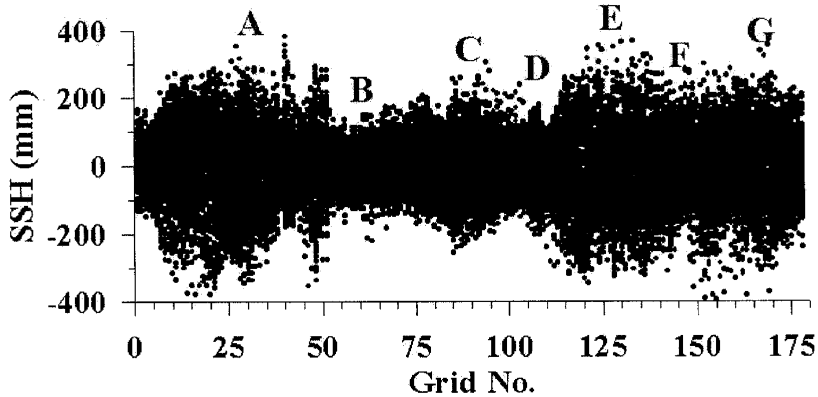

Fig. 2—Scatter diagrams of SSH for the years 1993-97 and for all the grids. A to G represents various selected regions presented in Fig. 1

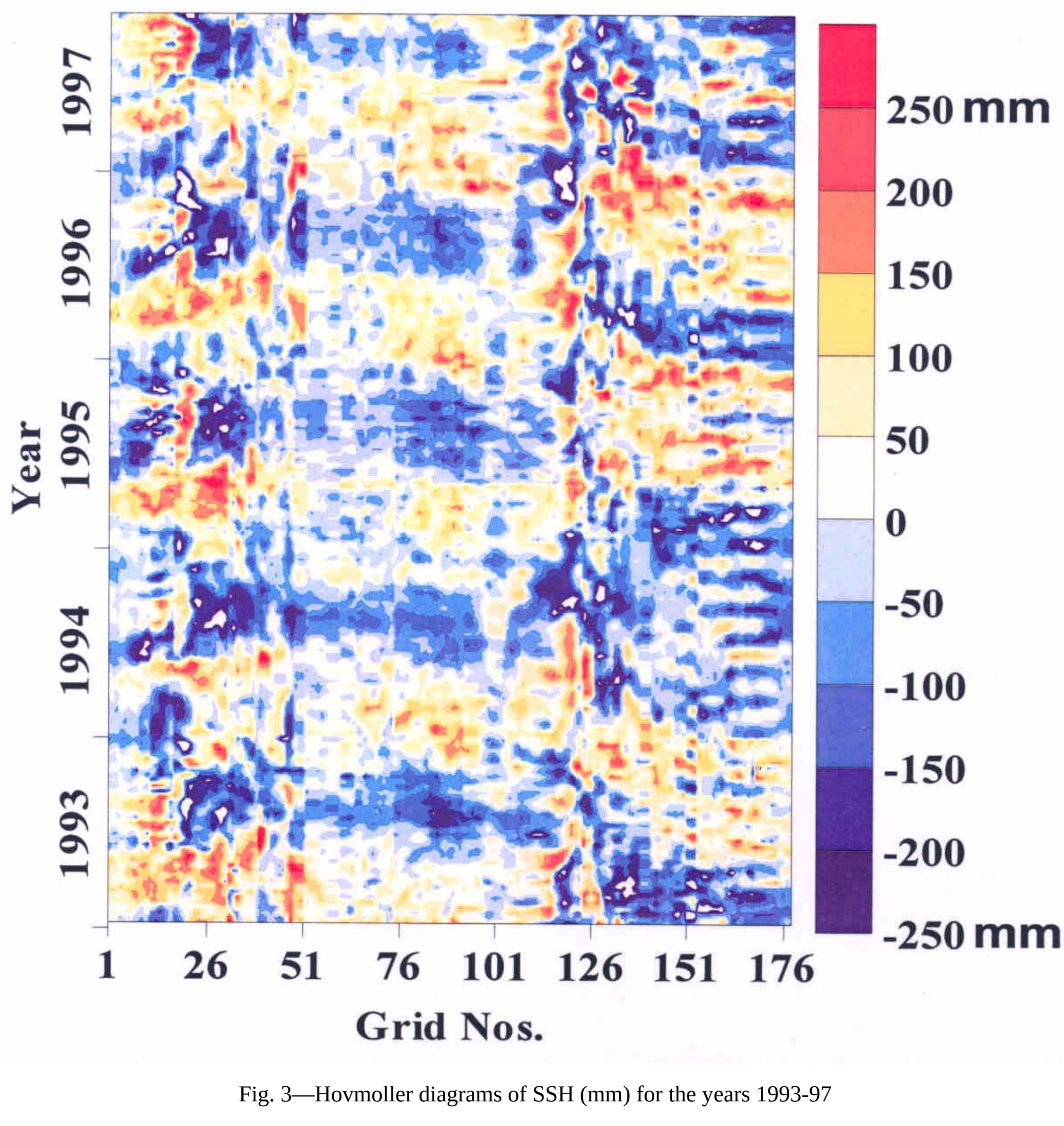

Fig. 3—Hovmoller diagrams of SSH (mm) for the years 1993-97

Sea during April, reached the head Bay (grid no. 140) by June.

Off the southern tip of India (grid no. 95), the high was observed during November. Studies have linked the appearance of this high off the southern tip of India and the formation of Laccadive high[1,9]. This wave further travels along the west coast of India and diffused by next April when it reached the northern Arabian Sea (grid no. 52).

Another notable observation was the formation of high SSH in the western Indian Ocean (grid 1) during February-May and propagated northward along the coastal boundaries of the Somalia and Arabia. This high SSH met with the high SSH, propagated from the eastern boundary, at the northern Arabian Sea (grid 52, i.e. off the Makran coast) by April and subsequently dissipated. Afterwards, a low was formed during May-August and another high during August-October in the western Indian Ocean. One of the notable observations is that unlike the high formed during February-May, the high during August-October did not propagate but remained off the Somalia coast confining to the grids 1 to 25. The above discussion revealed that the Makran coast acts as the meeting place of the both the incoming waves from western and eastern Arabian Sea.

In order to study the characteristics of waves in the coastal regions in detail, nine typical stations along the coastal belt were selected (grid nos. 1, 20, 55, 89, 100, 125, 145, 160, 178 in the regions A to G). In addition, two stations, representing central Arabian Sea (179) and Bay of Bengal (180) were also selected to compare the variability between coastal and deep oceanic regions. Time series of SSH was retrieved for these stations from the original data set. Wavelet decomposition method[10-12] was utilized to identify the embedded oscillations at all the stations (Fig. 4). The dominant periodic bands all along the coastal belt were ~30 days, 50-60 days, 3-4 months, 6-7 months and annual. Oscillations of 30-60 days periodicity can be grouped together, which is the band of intra-seasonal oscillation (ISO). Out of these, the annual wave had the maximum amplitude.

In the Indian Ocean, regions off Somalia (grids 1 to 20), between grids 1 and 20, marked differences were evident in the amplitude of sea level variability. Off Gulf of Aden (grid 20), all the frequency components were stronger (Fig. 4A) in accordance with the large scatter (Fig. 2). On the other hand, near the equator (grid 1), amplitudes of all components were very weak (-50 to 50 mm) thereby resulting minimum scatter. Off the Makran coast (Fig. 4B), all the frequency components contained lesser energy, as evident from the high frequency (wave height: –50 to 50 mm) and low frequency (wave height: -100 to 100 mm) components. This is in accordance with the minimum scatter in SSH observed in area B (Fig. 2). Off the west coast of India (Fig. 4C, grid 89), low frequency components (annual and nearly semi-annual) were stronger compared to that off Makran (grid 55) and off Sri Lanka (grid 100).

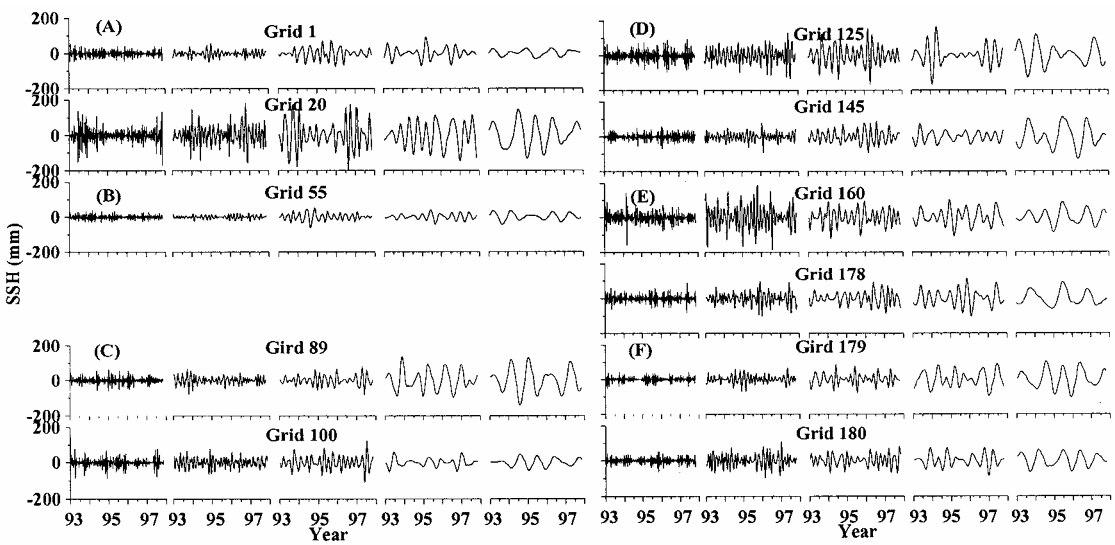

Fig. 4—Decomposed signals of SSH (mm) representing (A) western coastal Arabian Sea (Grid Nos. 1 and 20), (B) Makran coast (Grid No. 55), (C) eastern Arabian Sea coast (Grid Nos. 89 and 100), (D) off the east coast of India, and head of the Bay (Grid Nos. 125 and 145), (E) eastern Bay of Bengal coast (Grid Nos. 160 and 175) and (F) interior oceans (Grid Nos. 179 and 180)

Off the east coast of India (Fig. 4D, grid 125), all components were of nearly equal magnitudes. Moreover, higher frequency components were stronger compared to that off the west coast of India. A notable feature in the head of the Bay (grid 145) is the increase in amplitude with decrease in frequency.

Inside the Andaman Sea (Fig. 4E, grid 160), the amplitude of ISO was strong (> 100 mm) and of nearly equal magnitude with the other lower frequency components. It is to be noted that the Andaman Sea is an enclosed body and hence the local wind forcing may be responsible for the higher amplitude in this frequency band. However, off Sumatra (grid 178), oscillation with 16 months periodicity was observed instead of the annual periodicity.

In order to understand the characteristics of the waves in the interior Arabian Sea (grid 179) and Bay of Bengal (grid 180), two grids were selected (Fig. 4F). Major differences were that the ISO band contained more energy in the Bay of Bengal, whereas low frequency band contained more energy in the Arabian Sea. On the other hand, there were no significant variations compared with that of the coastal stations.

The analysis revealed that in the regions (off Gulf of Aden, southwest and east coast of India and eastern Bay of Bengal) of high spread in SSH, low frequency waves (>3 months) of high amplitude were significant. However, off Gulf of Aden and eastern Bay of Bengal, high frequency waves were also of equally important. On the other hand, in the regions of low scatter (Fig. 2), amplitude of low frequency components (>3 months) were conspicuously weak compared to other regions.

The oscillations found in this study were also reported earlier in the equatorial wave-guide and interior ocean[13-15] and which were attributed to the Kelvin, and Rossby waves, and mixed-Rossby-gravity waves. In addition, internal instabilities in the Ocean can also generate waves in the ISO band[14,15]. However, information on the characteristics of these waves along the coastal boundaries is extremely sparse. This study revealed the dominant harmonics in the SSH field which contained significant energy. These waves are very prominent in the entire coastal belt as well as in the deep-ocean. Moreover, the nature and spatial variability of these different wave bands are also brought out in this study. The results will be of use to enhance the understanding of various coastal processes linked with the coastally trapped waves, viz. mixed layer variability, eddies, circulation, meso-scale features, upwelling, sinking and sea level variability.

Acknowledgement

Authors are thankful to the TOPEX/POSEIDON team for providing the processed SSH data. The support and encouragement provided by the Director, NPOL is gratefully acknowledged here.

References

1 Shankar D & Shetye S R, On the dynamics of the Lakshadweep high and low in the southern Arabian Sea, *J Geophys Res (Oceans)*, 102 (1997) 12551-12562.

2 Shankar D, McCreary J P, Han W & Shetye S R, Dynamics of the east India coastal currents, 1, Analytic solutions forced by interior Ekman pumping and local alongshore winds, *J Geophys. Res (Oceans)*, 101 (1996) 13975-13992

3 Shankar D, Seasonal cycle of sea level and currents along the coast of India, *Cur Sci*, 78 (2000) 279-288.

4 Yu L, O'Brien J J & Yang J, On the remote forcing of the circulation in the Bay of Bengal, *J Geophys Res (Oceans)*, 96 (1991) 20449-20454.

5 Potemra J T, Luther M E. & O'Brien J J, The seasonal circulation of the upper ocean in the Bay of Bengal, *J Geophys Res (Oceans)* , 96 (1991) 12667-12683.

6 McCreary J, Kundu P K & Molinari R L, A numerical investigation of dynamics, thermodynamics and mixed-layer processes in the Indian Ocean, *Prog Oceanogr*, 31 (1993) 181-244.

7 Subrahmanyam B, Robinson I S, Blundell J R. & Challenor PG, Indian Ocean Rossby waves observed in TOPEX/POSEIDON altimeter data and in model simulations, *Int J Remote Sensing*, 22 (2001) 141-167.

8 Hareesh Kumar P V, Prasada Rao C V K, Swain J & Madhusoodanan P (2001) Intra-seasonal oscillation in the central Bay of Bengal during summer monsoon-99, *Cur Sci*, 80 (2001) 786-790.

9 Kindle J C & Thomson J D, The 26- and 50- day oscillations in the western Indian Ocean: model results, *J Geophys Res (Oceans)*, 94 (1989) 4721-4747.

10 Folland C K, Parker D E & Kraets F E, Worldwide marine temperature fluctuations 1856-1981, *Nature*, 310 (1984) 670-675.

11 Meyers S D, Kelly B G & O'Brien J J, An introduction to wavelet analysis in oceanography and meteorology with application in the dispersion of Yanai waves, *Mon Weather Rev*, 121 (1993) 2858-2866.

12 Mark M, Orthogonal wavelet analysis: Inter-annual variability in the sea surface temperature, *Bull Amer Meteor Soc*, 76 (1995) 2179-2186.

13 Moore D W & McCreary J P, Excitation of intermediate frequency equatorial waves at a western ocean boundary: With application to observations from the Indian Ocean, *J Geophys Res (Oceans)*, 95 (1990) 5129-5231.

14 Woodberry K E, Luther M E. & O'Brien J J, The wind-driven seasonal circulation in the southern tropical Indian Ocean, *J Geophys Res (Oceans)*, 94 (1989) 17985-18002.

15 Bruce J G, Kindle J C, Kantha L H, Kerling J L & Bailey J F, Recent observations and modeling in the Arabian Sea Laccadive High region, *J Geophys Res (Oceans)*, 103 (1988) 7593-7600.